Analyzing Continuous Conduction Mode Closed-Loop DC-DC Buck Converters with A Linear Method

Shih-Hsiung Twu
Department of Electrical Engineering
Chung Yuan Christian University
Chung-Li 32023, Taiwan
abraham@cycu.edu.tw

Li-Shan Ma
Department of Electrical Engineering
Chung Yuan Christian University
Chung-Li 32023, Taiwan
lsma@cycu.edu.tw

2022 25th International Conference on Mechatronics Technology (ICMT) | 978-1-6654-6195-5/22/$31.00 ©2022 IEEE | DOI: 10.1109/ICMT56556.2022.9997614

***Abstract*—In this paper, we will study the period 1 dynamics of the closed-loop dc-dc buck converters operating in continuous conduction mode (CCM) by a new theoretical method which is based on the state sequence flow charts proposed by the authors. In our investigation, the derived exact solutions of open-loop converters in CCM can be applied to analyze the period one dynamics of the closed-loop dc-dc buck converters when the feedback dynamic criterion is met. By this criterion equation, the switching time can be solved with numerical method faster. By this determined switching time, steady state time waves of closed-loop dc-dc buck converters operating in CCM can be calculated directly by open-loop derived exact solutions without transition simulations. Output ripple and average output voltages can be calculated within a period time simulations. The benefits of our study will provide a brand-new and precisely point of view to analyze DC-DC converters.**

Keywords—buck converter, dc-dc converter, continuous conduction mode (CCM), circuit modeling, closed-loop system, state sequence flow chart

I. INTRODUCTION

For dc-dc buck converters, the switching actions cause the exchange of two linear circuit systems in CCM, but it is a major obstacle to find the solutions of general open-loop and closed-loop dc-dc buck converters. The rich phenomena exhibited in the dc-dc buck converters will be explored via our study. There are many literatures are devoted to solve this switching converters including topology [1] and [2], linearized low frequency model [3]-[5], and linearized discrete time model [6]-[9], etc. In [10] and [11], the exact solutions of the open-loop buck converter are derived. By these derivations, the following main results are explored (1) The exact steady state and transient state solutions to open-loop converters operating in CCM are derived by the state sequence flow chart method for the first time. (2) The boundary of CCM and DCM, average output voltages and output voltage ripples are analyzed based on the exact solutions for the variation of all system parameters. In contrast, the previous some literatures were made only approximate analysis for partial system parameters. (3)This method can be applied to derive the exact periodic solutions of closed-loop buck converters furtherly. (4) The asymptotically periodic motions exhibit in open-loop buck converters and independent of effects due to initial conditions are proven theoretically for the first time. In this paper, the previous published results [11] about exact solutions of open-loop buck converter will be applied to analyze periodic one dynamics in CCM closed-loop DC-DC buck converters. Some results of closed-loop periodic one dynamics are adapted from unpublished content of [10]. However, duty-cycles with input voltages, output ripples and average output voltages of closed-loop buck converter are calculated and simulated for the first time. With our derived solutions, the nonlinear phenomena of switching dc-dc converters will be further explored precisely and simply in the future.

This paper is organized as follows. In the part one of section 2, we demonstrate the exact solutions for the open-loop dc-dc buck converters operating in CCM by [10] and [11]. The periodic one motions of CCM closed-loop buck converter are analyzed in the part 2 of section 2. In section 3, the simulation results are also presented to verify the theoretical investigations. At last, conclusions are given in section 4.

II. ANALYSIS OF DC-DC BUCK CONVERTER

A. *Exact Solutions of Open-Loop Buck Converter for CCM by the Linear Method* [10] and [11]

Fig.1 shows an open-loop dc-dc buck (step down) converter.

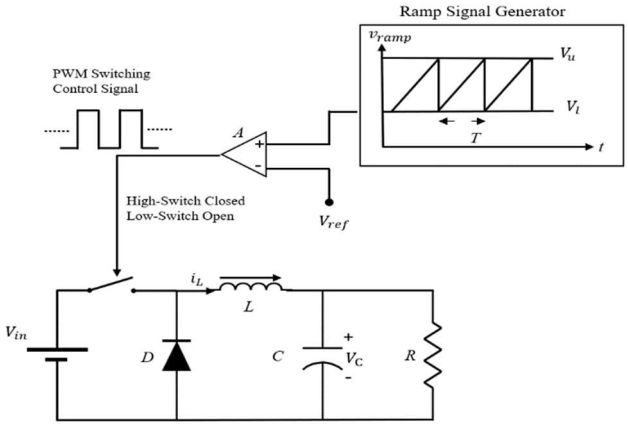

Fig.1 Block diagram of the open-loop buck converter.

Due to a dc reference voltage and a sawtooth voltage shown in Fig. 2, the periodic one PWM will be generated. The period one PWM determined the switch on or off i.e. which system state solutions will be used in our derivations.

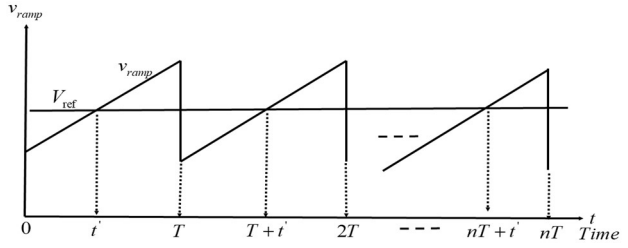

Fig. 2 The sawtooth and dc reference voltages in open-loop dc-dc converter.

The dynamic of dc-dc buck converters operating on CCM can be described as: [12]

$$\frac{d}{dt}\begin{bmatrix} V_C(t) \\ i_L(t) \end{bmatrix} = \begin{bmatrix} -1/(RC) & 1/C \\ -1/L & 0 \end{bmatrix}\begin{bmatrix} V_C(t) \\ i_L(t) \end{bmatrix}, \; nT \le t < nT + t', \quad (1a)$$

$$\frac{d}{dt}\begin{bmatrix} V_C(t) \\ i_L(t) \end{bmatrix} = \begin{bmatrix} -1/(RC) & 1/C \\ -1/L & 0 \end{bmatrix}\begin{bmatrix} V_C(t) \\ i_L(t) \end{bmatrix} + \begin{bmatrix} 0 \\ V_{in}/L \end{bmatrix}, \quad nT + t' \le t < (n+1)T. \quad (1b)$$

The solutions for the systems can be list as following:

$$\begin{pmatrix} V_C(t) \\ i_L(t) \end{pmatrix} = e^{-\alpha(t-t_0)}[I\cos\omega(t-t_0) + A\sin\omega(t-t_0)]\begin{pmatrix} V_0 \\ i_0 \end{pmatrix}, \quad nT \le t < nT + t', \quad (2a)$$

$$\begin{pmatrix} V_C(t) \\ i_L(t) \end{pmatrix} = \begin{pmatrix} V_o(t) \\ i_o(t) \end{pmatrix} + e^{-\alpha(t-t_0)}[I\cos\omega(t-t_0) + A\sin\omega(t-t_0)]\cdot \begin{pmatrix} v_0 - V_{in} \\ i_0 - V_{in}/R \end{pmatrix}, \; nT + t' \le t < (n+1)T, \quad (2b)$$

where $\alpha = 1/2RC$, $w = \sqrt{1/LC - \alpha^2}$, $A = \begin{pmatrix} -\alpha/\omega & 1/(C\omega) \\ -1/(L\omega) & \alpha/\omega \end{pmatrix}$ and supposing that $\frac{1}{LC} - \alpha^2 > 0$

(1) *State sequence flow chart*

With the state sequence flow charts from the dynamic equations of open-loop buck converters, the exact solutions for CCM can be derived at first. Then the boundary of CCM and DCM, average output voltages and output ripples due to the variation of system parameters will be analyzed with the exact solutions [10] and [11]. The asymptotically periodic motion exhibited in open-loop buck converters are also proven. It provides the mathematical base of further analysis for open-loop and closed-loop buck converters.

At First, the states of open-loop converters in CCM can be presented as follows from the equations (1) and (2):

When $nT \le t \le nT + t'$,

$$\begin{pmatrix} V_C(t) \\ i_L(t) \end{pmatrix} = \begin{pmatrix} k_1(t) & k_2(t) \\ k_3(t) & k_4(t) \end{pmatrix}\begin{pmatrix} V_C(nT\,) \\ i_L(nT) \end{pmatrix} = A_{TSW}(t)\begin{pmatrix} V_C(nT) \\ i_L(nT) \end{pmatrix}, \quad (3a)$$

with $A_{TSW}(t) = \begin{pmatrix} k_1(t) & k_2(t) \\ k_3(t) & k_4(t) \end{pmatrix}$;

when $nT + t' \le t \le (n+1)T$,

$$\begin{pmatrix} V_C(t) \\ i_L(t) \end{pmatrix} = \begin{pmatrix} k_6(t) & k_7(t) \\ k_9(t) & k_{10}(t) \end{pmatrix}\begin{pmatrix} V_C(nT+t') \\ i_L(nT+t') \end{pmatrix} + \begin{pmatrix} k_5(t) \\ k_8(t) \end{pmatrix}V_{in} = A_{SWT}(t)\begin{pmatrix} V_C(nT+t') \\ i_L(nT+t') \end{pmatrix} + B_{SWT}(t)V_{in}, \quad (3b)$$

with $A_{SWT}(t) = \begin{pmatrix} k_6(t) & k_7(t) \\ k_9(t) & k_{10}(t) \end{pmatrix}$ $B_{SWT}(t) = \begin{pmatrix} k_5(t) \\ k_8(t) \end{pmatrix}$,

where,

$$k_1(t) = e^{-\alpha(t-nT)}\left(\frac{-\alpha}{\omega}Sin\omega(t-nT) + Cos\omega(t-nT)\right),$$

$$k_2(t) = e^{-\alpha(t-nT)}\left(\frac{1}{C\omega}\right)Sin\omega(t-nT),$$

$$k_3(t) = e^{-\alpha(t-nT)}\frac{-1}{L\omega}Sin\omega(t-nT),$$

$$k_4(t) = e^{-\alpha(t-nT)}\left(\frac{\alpha}{\omega}Sin\omega(t-nT) + Cos\omega(t-nT)\right),$$

$$k_5(t) = \{1 - e^{-\alpha(t-(nT+t'))}[Cos\omega(t-(nT+t')) + (\frac{1}{RC\omega} - \frac{\alpha}{\omega})\cdot Sin\omega(t-(nT+t'))]\},$$

$$k_6(t) = e^{-\alpha(t-(nT+t'))}[(\frac{-\alpha}{\omega})Sin\omega(t-(nT+t')) + Cos\omega(t-(nT+t'))],$$

$$k_7(t) = e^{-\alpha(t-(nT+t'))}[(\frac{1}{C\omega})Sin\omega(t-(nT+t'))],$$

$$k_8(t) = \frac{1}{R}\{1 - e^{-\alpha(t-(nT+t'))}[Cos\omega(t-(nT+t')) + (\frac{\alpha}{\omega} - \frac{R}{L\omega})\cdot Sin\omega(t-(nT+t'))],$$

$$k_9(t) = e^{-\alpha(t-(nT+t'))}[\frac{-1}{L\omega}Sin\omega(t-(nT+t'))]$$

$$k_{10}(t) = e^{-\alpha(t-(nT+t'))}[(\frac{\alpha}{\omega})Sin\omega(t-(nT+t')) + Cos\omega(t-(nT+t'))].$$

By letting $t = nT + t'$ in equation (3a) and $t = (n+1)T$ in equation (3b), we obtain

$$\begin{pmatrix} V_C(nT+t') \\ i_L(nT+t') \end{pmatrix} = \begin{pmatrix} k_1 & k_2 \\ k_3 & k_4 \end{pmatrix}\begin{pmatrix} V_C(nT) \\ i_L(nT) \end{pmatrix} = A_{TSW}\begin{pmatrix} V_C(nT) \\ i_L(nT) \end{pmatrix}, \quad (4a)$$

$$\begin{pmatrix} V_C((n+1)T) \\ i_L((n+1)T) \end{pmatrix} = \begin{pmatrix} k_6 & k_7 \\ k_9 & k_{10} \end{pmatrix}\begin{pmatrix} V_C(nT+t') \\ i_L(nT+t') \end{pmatrix} + \begin{pmatrix} k_5 \\ k_8 \end{pmatrix}V_{in} = A_{SWT}\begin{pmatrix} V_C(nT+t') \\ i_L(nT+t') \end{pmatrix} + B_{SWT}V_{in}, \quad (4b)$$

where $k_i = k_i(nT + t')$, $i = 1,2,3,4$,
$k_i = k_i((n+1)T)$, $i = 5,6,7,8,9,10$,
$A_{TSW} = A_{TSW}(nT + t')$,
$A_{SWT} = A_{SWT}((n+1)T)$ and $B_{SWT} = B_{SWT}((n+1)T)$.

From equation (4), when these quantities $V_C(nT)$, $i_L(nT)$, $V_C(nT + t')$ and $i_L(nT + t')$ are known, the exact solutions to our system will be obtained.

In the following, a new method for deriving the exact formulas of $V_C(nT)$, $i_L(nT)$, $V_C(nT + t')$ and $i_L(nT + t')$ in terms of $V_C(0)$, $i_L(0)$ and V_{in} will be presented. At first, we consider the *state sequence flow chart* proposed by the authors will be drawn from equation (4). In open loop case, the exact solution will be influenced by three factors $V_C(0)$, $i_L(0)$ and V_{in}. We can draw the sequence flow chart by observing the relationship between the $V_C(0)$, $i_L(0)$ and V_{in} with the parameters k_i $i = 1...10$ as shown in Fig. 3.

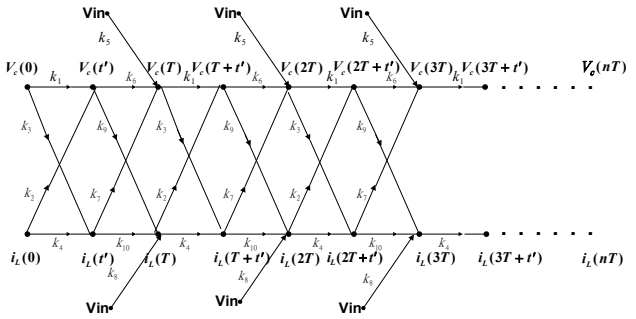

Fig. 3 The CCM state sequence flow chart.

(2) Motions caused by initial conditions

When only the initial condition $V_C(0)$ is considered, the state sequence flow chart shown in Fig. 3 can be redrawn as Fig. 4.

From Fig. 4, the relationship between the subsequent state sequence variables $\left[V_C((n+1)T+t')\ i_L((n+1)T+t')\right]^T$ and $\left[V_C(nT+t')\ i_L(nT+t'))\right]^T$ can be presented by the following linear homogeneous difference equation:

$$\begin{pmatrix} V_C((n+1)T+t') \\ i_L((n+1)T+t') \end{pmatrix} = A_{CMSW} \begin{pmatrix} V_C(nT+t') \\ i_L(nT+t') \end{pmatrix},\ n \ge 0, \tag{5}$$

where $A_{CMSW} = \begin{pmatrix} k_6k_1 + k_9k_2 & k_7k_1 + k_{10}k_2 \\ k_9k_4 + k_6k_3 & k_{10}k_4 + k_7k_3 \end{pmatrix}$,

with initial condition

$$\begin{pmatrix} V_C(t') \\ i_L(t') \end{pmatrix} = \begin{pmatrix} k_1 \\ k_3 \end{pmatrix} V_C(0)\,.$$

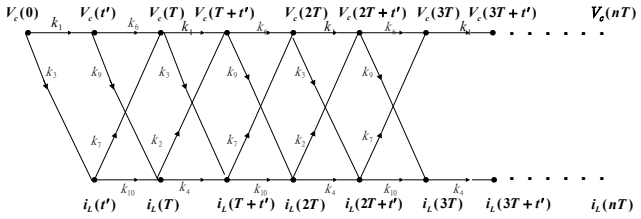

Fig. 4 The CCM state sequence flow chart with initial condition $V_C(0)$.

Then, the solutions to equation (5) can be solved by

$$\begin{pmatrix} V_C(nT+t') \\ i_L(nT+t') \end{pmatrix} = A_{CMSW}^n \begin{pmatrix} k_1 \\ k_3 \end{pmatrix} V_C(0)\,. \tag{6}$$

Similarly, from Fig. 4, the relationship between the subsequent state sequence variables $\left[V_C[(n+1)T]\ i_L[(n+1)T]\right]^T$ and $\left[V_c(nT)\ i_L(nT)\right]^T$ can also be represented by the following linear homogeneous difference equation:

$$\begin{pmatrix} V_C((n+1)T) \\ i_L((n+1)T) \end{pmatrix} = A_{CMT} \begin{pmatrix} V_C(nT) \\ i_L(nT) \end{pmatrix},\ n \ge 1\,, \tag{7}$$

where $A_{CMT} = \begin{pmatrix} k_1k_4 + k_3k_7 & k_4k_7 + k_2k_6 \\ k_3k_{10} + k_1k_9 & k_4k_{10} + k_2k_9 \end{pmatrix}$,

with initial condition

$$\begin{pmatrix} V_C(T) \\ i_L(T) \end{pmatrix} = \begin{pmatrix} k_1k_6 + k_3k_7 \\ k_1k_9 + k_3k_{10} \end{pmatrix} V_C(0)\,.$$

Then, the solutions to equation (7) can be solved by

$$\begin{pmatrix} V_C(nT) \\ i_L(nT) \end{pmatrix} = A_{CMT}^n \begin{pmatrix} k_1k_6 + k_3k_7 \\ k_1k_9 + k_3k_{10} \end{pmatrix} V_C(0)\,. \tag{8}$$

It is obvious that from equation (6)

$$\lim_{n\to\infty} \begin{pmatrix} V_C(nT+t') \\ i_L(nT+t'^{\mathrm{n}}) \end{pmatrix} = \lim_{n\to\infty} A_{CMSW}^n \begin{pmatrix} k_1 \\ k_3 \end{pmatrix} V_C(0) \to \vec{0}\,, \tag{9}$$

if the norms of eigenvalues of A_{CMSW} are all less than 1.

Similarly, from equation (8),

$$\lim_{n\to\infty} \begin{pmatrix} V_C(nT) \\ i_L(nT) \end{pmatrix} = \lim_{n\to\infty} A_{CMT}^n \begin{pmatrix} k_1k_6 + k_3k_7 \\ k_1k_9 + k_3k_6 \end{pmatrix} V_C(0) \to \vec{0}\,, \tag{10}$$

if the norms of eigenvalues of A_{CMT} are all less than 1.

Equations (9) and (10) mean that the amplitudes of $\left[V_C(nT) i_L(nT)\right]^T$ and $\left[V_C(nT+t') i_L(nT+t')\right]^T$ due to initial condition $V_C(0)$ will decay to zero vectors asymptotically.

We can also prove the motions caused by the initial condition $i_L(0)$ will decay to zero vector in the same way. In summary, the vibrations due to initial conditions $V_C(0)$ and $i_L(0)$ will go to zero vectors as time goes to infinity.

(3) Exact solutions due to the input voltage

For the case of the input voltage V_{in} is considered, the state sequence flow chart can be redrawn as in Fig. 5.

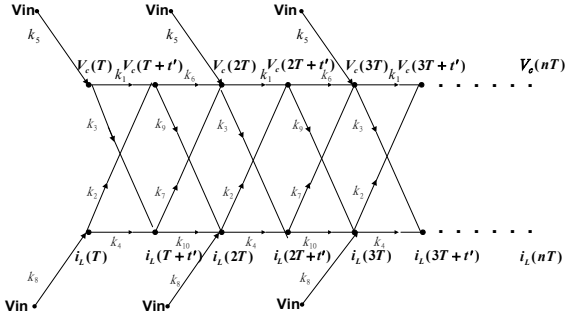

Fig. 5 The CCM state sequence flow chart with input variable V_{in} .

At first, from Fig. 5, the relationship between the subsequent state sequence variables $\left[V_C((n+1)T+t')\ i_L((n+1)T+t')\right]^T$ and $\left[V_C(nT+t')\ i_L(nT+t')\right]^T$ can be represented by the following linear homogeneous difference equation:

$$\begin{pmatrix} V_C((n+1)T+t') \\ i_L((n+1)T+t') \end{pmatrix} = A_{CMSW} \begin{pmatrix} V_C(nT+t') \\ i_L(nT+t') \end{pmatrix} + B_{CMSW} V_{in}, n \ge 1, \tag{11}$$

where $B_{CMSW} = \begin{pmatrix} k_5k_1 + k_8k_2 \\ k_8k_4 + k_5k_3 \end{pmatrix}$,

with initial condition $\begin{pmatrix} V_C(T+t') \\ i_L(T+t') \end{pmatrix} = \begin{pmatrix} k_5k_1 + k_8k_2 \\ k_5k_3 + k_8k_4 \end{pmatrix} V_{in}$.

From equation (11), the solutions to state sequence variables $\left[V_C(nT+t')\ i_L(nT+t')\right]^T$ in terms of V_{in} is obtained by

$$\begin{pmatrix} V_C(nT+t') \\ i_L(nT+t') \end{pmatrix} = A_{CMSW}^{n-1} \begin{pmatrix} V_C(T+t') \\ i_L(T+t') \end{pmatrix} + \sum_{i=0}^{n-2} A_{CMSW}^i B_{CMSW} V_{in}. \tag{12}$$

Since $\lim_{n\to\infty}\left(A_{CMSW}^{n-1}\right) \to 0$ if the norms of the eigenvalues

of A_{CMSW} are all less than 1. It can be concluded that $\left[V_C(nT+t')\ i_L(nT+t')\right]^T$ will converge to a constant vector

$$\lim_{n\to\infty}\begin{pmatrix}V_C(nT+t')\\ i_L(nT+t')\end{pmatrix}=\lim_{n\to\infty}\sum_{i=0}^{n-2}A_{CMSW}^{i}B_{CMSW}V_{in} \quad (13)$$
$$=(I-A_{CMSW})^{-1}B_{CMSW}V_{in}.$$

Similarly, from Fig. 6, the relationship between the successive state sequence variables $\left[V_C(nT)\ i_L(nT)\right]^T$ and $\left[V_C((n+1)T]\ i_L((n+1)T)\right]^T$ in term of V_{in} can be represented by the following homogeneous equation:

$$\begin{pmatrix}V_C((n+1)T\\ i_L((n+1)T\end{pmatrix}=A_{CMT}\begin{pmatrix}V_C(nT)\\ i_L(nT)\end{pmatrix}+B_{CMT}V_{in},\ n\ge 1, \quad (14)$$

with initial condition $\begin{pmatrix}V_C(T)\\ i_L(T)\end{pmatrix}=\begin{pmatrix}k_5\\ k_8\end{pmatrix}V_{in}$.

Via equation (14), the solutions to state sequence variables $\left[V_C(nT)\ i_L(nT)\right]^T$ in terms of V_{in} is obtained by

$$\begin{pmatrix}V_C(nT)\\ i_L(nT)\end{pmatrix}=A_{CMT}^{n-1}\begin{pmatrix}V_C(T)\\ i_L(T)\end{pmatrix}+\sum_{i=0}^{n-2}A_{CMT}^{i}B_{CMT}V_{in}. \quad (15)$$

Since $\lim_{n\to\infty}A_{CMT}^{n-1}\to 0$, if the norms of the eigenvalues of A_{CMT} are all less than 1. It can be concluded that

$$\lim_{n\to\infty}\begin{pmatrix}V_C(nT)\\ i_L(nT)\end{pmatrix}=\lim_{n\to\infty}\sum_{i=0}^{n-2}A_{CMT}^{i}B_{CMT}V_{in}=(I-A_{CMT})^{-1}B_{CMT}V_{in}. \quad (16)$$

The equations (13) and (16) mean that the state sequences $\left[V_C(nT)\ i_L(nT)\right]^T$ and $\left[V_C(nT+t')\ i_L(nT+t')\right]^T$ will converge to the constant vectors $(I-A_{CMT})^{-1}B_{CMT}V_{in}$ and $(I-A_{CMSW})^{-1}B_{CMSW}V_{in}$, respectively. In the other words, the system's state $\left[V_C(t)\ i_L(t)\right]^T$ will converge to periodic motions asymptotically. It is emphasized that the periodicity of $\left[V_C(t)\ i_L(t)\right]^T$ in open-loop buck converters is proven for the first time.

The exact steady-state solutions to our system can be derived by substituting equations (16) and (13) into (4a) and (4b):

For $nT\le t\le nT+t'$,

$$\begin{pmatrix}V_C(t)\\ i_L(t)\end{pmatrix}=A_{TSW}(t)\begin{pmatrix}V_C(nT)\\ i_L(nT)\end{pmatrix}=A_{TSW}(t)(I-A_{CMT})^{-1}B_{CMT}V_{in}, \quad (17a)$$

For $nT+t'\le t\le (n+1)T$,

$$\begin{pmatrix}V_C(t)\\ i_L(t)\end{pmatrix}=A_{SWT}(t)\begin{pmatrix}V_C(nT+t')\\ i_L(nT+t')\end{pmatrix}+B_{SWT}(t)V_{in}$$
$$=A_{SWT}(t)(I-A_{CMSW})^{-1}B_{CMSW}V_{in}+B_{SWT}(t)V_{in}. \quad (17b)$$

B. Analysis of Closed-Loop Buck Converter with Periodic one for CCM

In this section, we will introduce the closed-loop dc-dc buck converters firstly. Then, we will derive a simple condition or criterion for period one motions in the closed-loop buck converters operating in CCM by our proposed new methods in last section. By this criterion, the switching time can be solved. Then, the switching times of period one motions respect to different input voltages can be solved too. By these switching times, the duty cycles can be calculated for different input voltages. Furthermore, the output ripples and output voltages can be determined only by one period simulation time.

Fig. 6 shows the block diagram of a closed-loop buck regulator that uses a PWM circuit to generate the switching wave for adjudging the duty cycle. In Fig 6, the comparison signal V_{CO} is

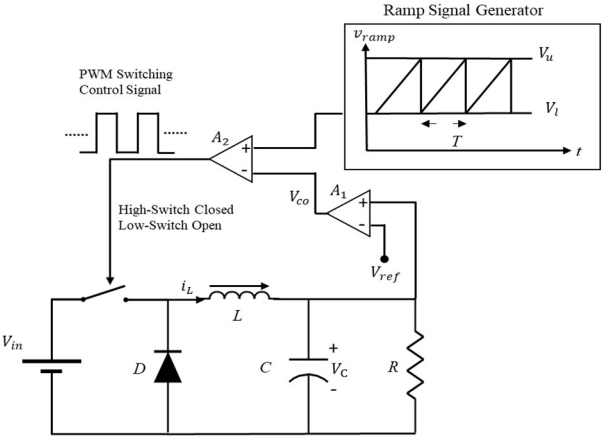

Fig.6 Block diagram of the closed-loop buck converter.

$$V_{CO}(t)=a\ (V_C(t)-V_{ref}), \quad (18)$$

and the ramp voltage is

$$V_{ramp}(t)=V_l+(V_u-V_l)t/T. \quad (19)$$

In the following, we will derive the condition of period one motions in CCM for closed-loop buck converter. The procedures of derivation in this case is the same as that of the open-loop by adding the following condition

$$V_{CO}(nT+t')-V_{ramp}(nT+t')=a\left[(V_C(nT+t')-V_{ref})\right]-V_{ramp}=0. \quad (20)$$

Condition (20) is used for determination of switching time t'. That is, the criterion of period one motions of closed-loop buck converters in CCM can be rewrite as the following criterion:

$$\begin{aligned}&V_{CO}(nT+t')-V_{ramp}(nT+t')\\ &=a\left[V_C(nT+t')-V_{ref}\right]-V_{ramp}(nT+t')\\ &=a\left[\begin{bmatrix}1 & 0\end{bmatrix}(I-A_{CMSW})^{-1}B_{CMSW}V_{in}-V_{ref}\right]-(V_l+\frac{V_u-V_l}{T}t')=0.\end{aligned} \quad (21)$$

III. Simulation Verification

In this section, the computer simulations will be given to verify the theoretical results including open-loop and closed loop derived solutions.

A. Case1: Open-Loop Buck Converter for CCM

In the following, we present an example to verify the previous derivations in part A of section 2. Fig 7 shows the transition simulation results due to $V_{in}=33V$, $V_C(0)=18V$, $i_L(0)=1A$, $R=22, L=20mH, C=47uF$ and $T=400us$ are given. The parameters of the PWM circuit are V_{ref}=5, V_u=8.4, and V_l=3. In other words, the duty cycle

$D = 0.629$ in the open-loop. In Fig. 7, it can be observed, the transition dynamics caused by the initial conditions $V_C(0)$ and $i_L(0)$ will decay to zero and the V_C(t) and i_L(t) will go to asymptotically periodic motions when time goes infinity.

In Fig.8 and Fig. 9, by derived solutions with input $V_{in} = 33V$, the steady-state time waveforms and phase portrait can be verified.

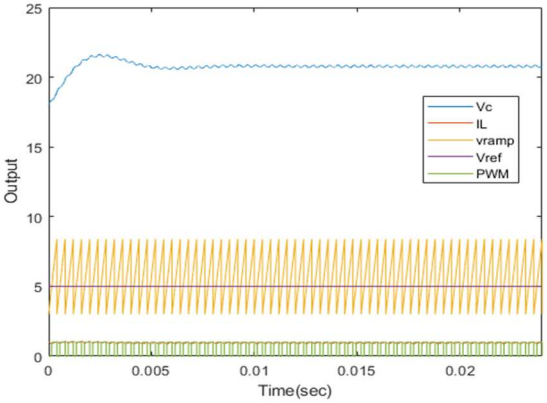

Fig.7 The CCM open-loop transient waveforms by the derived solutions with input $V_{in} = 33V$ and initial conditions $V_C(0)$ =18V and $i_L(0) = 1A$.

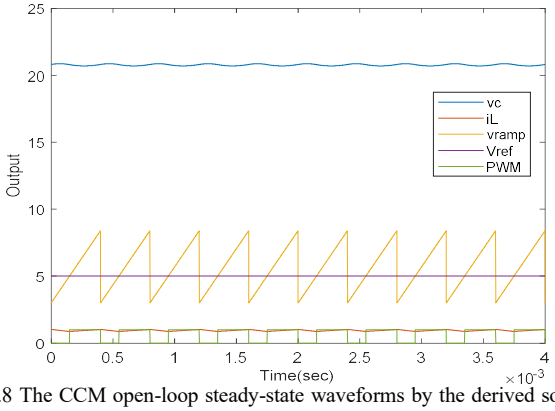

Fig.8 The CCM open-loop steady-state waveforms by the derived solutions with input $V_{in} = 33V$.

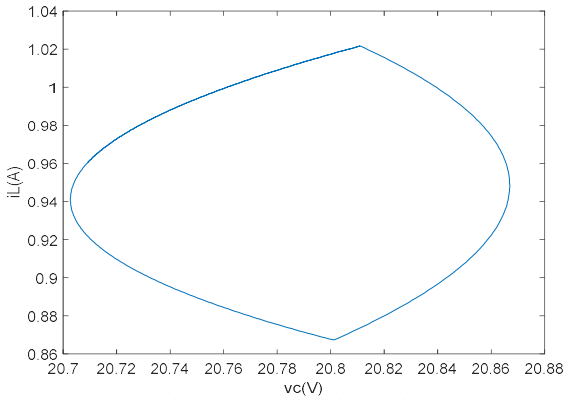

Fig.9 The CCM open-loop phase portrait by the derived solutions with input $V_{in} = 33V$.

B. *Case2: Closed-Loop Buck Converter with Periodic one for CCM*

In the following, we present an example to verify the previous derivation in part B of section 2. In this case, $R = 22, L = 20mH, C = 47uF$ and $f = 2.5kHz$ are given. The parameters of the PWM circuit are V_{ref}=11.3, a=8.4, V_u=8.4, and V_l=3.8.

(1) Simulations of CCM closed-loop periodic one steady-state waveforms

Fig 10 shows the steady state simulation results due to $V_{in} = 16V$. By (21), the switching time 1.0315×10^{-4} can be solved. By (17) and this switching time, the steady state waveforms can be simulated.

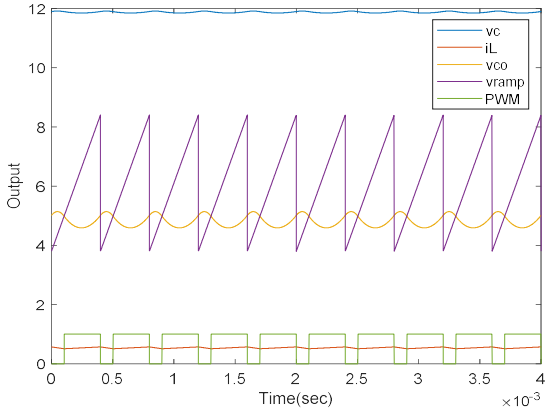

Fig.10 The CCM closed-loop periodic one steady-state waveforms by the derived solutions with input $V_{in} = 16V$ and solved switching time 1.0315×10^{-4} .

(2) Simulations of periodic one duty cycles for different input voltages

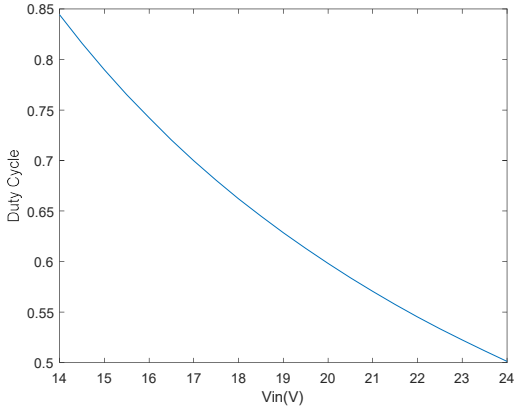

Fig.11 The CCM closed-loop periodic one duty cycles for different input voltages.

(3) Simulations of output ripples and average output voltages

By solved switching times and one period simulations, the output ripples and average output voltages can be calculated for different input voltages. The formula for simulating steady-state average output voltage for CCM closed-loop period one waveforms can be expressed by

$$V_{AVE} = \frac{1}{2}(\max(V_C(t)) + \min(V_C(t))),\ 0 \le t \le T\,. \quad (22)$$

On the other hand, The formula for simulating the steady-state output ripple for CCM closed-loop period one waveforms can be represented by

$$V_{rip} = \max(V_C(t)) - \min(V_C(t)),\ 0 \le t \le T. \quad (23)$$

Base on simulation formulae (22) and (23) and the variation of system parameter V_{in}, the output ripple voltages and average output voltages can be simulated as shown in the Fig. 12 and Fig.13, respectively.

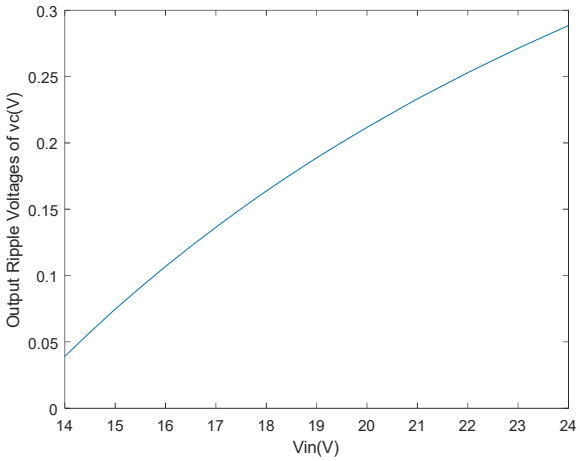

Fig.12 The CCM closed-loop periodic one output ripple voltages for different input voltages.

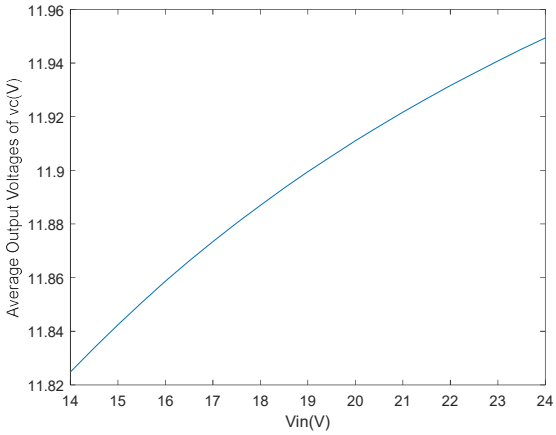

Fig.13 The CCM closed-loop periodic one average output voltages for different input voltages.

IV. Conclusions

In this paper, the authors have applied the derived exact solutions of CCM open-loop buck converters to analyze the period 1 dynamics of closed-loop CCM buck converters. By the concept of state sequence flow chart and only linear system theory, our derivations has been introduced. The open-loop derived exact solutions have been utilized to study the period 1 dynamics of the closed-loop dc-dc buck converters when the feedback dynamic criterion equation is satisfied. With the derived period one criterion equation, the switching time has been solved to simulate steady state time waves, to determine the steady-state duty cycle, to calculate output ripple and average output voltage with one period simulation. The new method proposed in this paper is not only simple but also applicable to practical design for dc-dc buck converters, because the period 1 dynamics in the closed-loop dc-dc buck converters for all parameters can be exactly calculated by proposed new theoretical method rather than some previous analysis methods just for partial parameters only.

References

[1] M. Touhami, G. Despesse and F. Costa, "A New Topology of DC–DC Converter Based on Piezoelectric Resonator," in *IEEE Transactions on Power Electronics*, vol. 37, no. 6, pp. 6986-7000, June 2022.

[2] M.Z. Hossain, N.A. Rahim, Jeyraj a/l Selvaraj, "Recent Progress and Development on Power DC-DC Converter Topology, Control, Design and Applications: A review, " in *Renewable and Sustainable Energy Reviews*, vol. 81, part 1, pp. 205-230, Jan. 2018.

[3] G. W. Wester and R. D. Middlebrook, "Low-Frequency Characterization of Switched dc-dc Converters," in *IEEE Transactions on Aerospace and Electronic Systems*, vol. AES-9, no. 3, pp. 376-385, May 1973.

[4] S. Kapat and P. T. Krein, "A Tutorial and Review Discussion of Modulation, Control and Tuning of High-Performance DC-DC Converters Based on Small-Signal and Large-Signal Approaches," in *IEEE Open Journal of Power Electronics*, vol. 1, pp. 339-371, 2020.

[5] D. Yan *et al*., "Review of General Modeling Approaches of Power Converters," in *Chinese Journal of Electrical Engineering*, vol. 7, no. 1, pp. 27-36, March 2021.

[6] C. K. Tse and K. M. Adams. "Qualitative Analysis and Control of a DC-DC Buck Converter Operating in Discontinuous Mode," *Journal of Electrical and Electronics Engineer*, vol. 10, no. 3, pp. 228-239, Spet. 1990.

[7] M. di Bernardo and F. Vasca, "Discrete-Time Maps for the Analysis of Bifurcations and Chaos in DC/DC Converters," in *IEEE Transactions on Circuits and Systems I: Fundamental Theory and Applications*, vol. 47, no. 2, pp. 130-143, Feb. 2000.

[8] Leng Zhaoxia, Liu Qingfeng, Sun Jinkun, and Wang Huamin, "A Discrete Modeling Approach for Buck Converter, " *Physics Procedia*, vol. 24, part A, pp. 710-716, Feb. 2012.

[9] Iqbal, Sajid, Kashif Ali Khan, and Shahid Iqbal. "Understanding Chaos Using Discrete-Time Map for Buck Converter." *3rd Chaotic Modelling and Simulation International Conference (CHAOS 2010)*, June 2010.

[10] Li-Shan Ma, "A New Method for Analyzing DC-DC Buck Converters," M.S. Thesis, Department of Electrical Engineering of Chung Yuan Christian University, Chung Li, Jun., 1997. [Online]. Available Record:https://cylis.lib.cycu.edu.tw/record=b1171784~S1*cht

[11] Shih Hsiuag Twu and Li-Shan Ma, "A New Method for Analyzing Open-Loop DC-DC Buck Converters," *Proceedings of the 13th T.V.E.* Conference, R.O.C., vol. 3, pp.236-272, May, 1998.

[12] E. Fossas and G. Olivar, "Study of Chaos in the Buck Converter," in *IEEE Transactions on Circuits and Systems I: Fundamental Theory and Applications*, vol. 43, no. 1, pp. 13-25, Jan. 1996.